CrossMark

ORIGINAL PAPER

The last Vesuvius eruption in March 1944: reconstruction of the eruptive dynamic and its impact on the environment and people through witness reports and volcanological evidence

Elena Cubellis[1] · Aldo Marturano[1] · Lucia Pappalardo[1]

Abstract Mount Vesuvius last erupted in March 1944. The eruption began with a modest effusive activity (18–21 March, phase I) and then moved on to a lava-fountain phase (21–22 March, phase II) that quickly culminated in a 24-h paroxsmal phase (22–23 March, phase III), during which the eruptive column reached its maximum altitude and ash carried by the wind was deposited at distances of up to 500 km from the volcano. Subsequently (phase IV), the ash cloud reached altitudes not exceeding 2 km above the crater and the explosions became discontinuous, alternating with frequent tremors. From April 7th the vent remained permanently closed. Since then, the current period of quiescence may be said to have begun. In our study we present a detailed geochemical study of the volcanic products emitted throughout the stages of the eruption, including an extreme distal ash sample, collected at the time of the eruption in Albania (Devoli) by the geologist Antonio Lazzari. The results indicate that magmatic differentiation took place in two crystallization stages under different temperature and pressure. Moreover, through the use of a numerical model of volcanic ash dispersion in the atmosphere as well as the collection of new witness accounts, we inferred the maximum height reached by the eruptive column (>8–10 km above the crater) as well as its impact on the environment and people, suggesting that the damage in the area and even the number of the victims could be higher than accepted until now.

Keywords 1944 Vesuvius eruption · Explosive eruption · Volcanic ash · Volcanic risk

✉ Lucia Pappalardo
   lucia.pappalardo@ingv.it

[1] Sezione di Napoli - Osservatorio Vesuviano, Istituto Nazionale di Geofisica e Vulcanologia (INGV), via Diocleziano 328, Naples, Italy

🖄 Springer

1 Introduction

The last eruption of Vesuvius [latitude (dd): 40.82, longitude (dd): 14.43, elevation (m): 1281] in March 1944 closed a 300-year-long period of intense eruptive activity that began immediately after the 1631 AD sub-plinian event and was characterized by moderately explosive eruptions and effusive activity (Arrighi et al. 2001; Scandone et al. 2008). The 1944 eruption was described in detail by the director of Vesuvius Observatory Prof. Giuseppe Imbò (1949a, b) who observed and monitored the eruption from the observatory located on the western slope of the volcano at an altitude of 608 m. The eruption began with a modest effusive activity and then moved on to a lava-fountain phase that quickly culminated in a paroxysmal phase, during which the eruptive column reached its maximum altitude (more than 5 km) and the ash carried by the wind arrived at distances exceeding 470 km eastward from Vesuvius.

After 70 years, the eruption is still present in the memory of people living in the Vesuvian area, who were direct victims of the event, but also of those who lived in the area affected by the ash cloud not only in Campania, but also in the regions of Molise, Basilicata and Puglia.

In this paper we perform a magma evolution model based on the geochemical compositions (concentration of major and volatile elements) of products (minerals and volcanic glass) emitted throughout the stages of the eruption in order to reconstruct pre- and syn-eruptive magmatic processes. Moreover, through the use of a numerical model of volcanic ash dispersion in the atmosphere as well as the collection of new accounts from witnesses, we infer the eruptive mechanism and its impact on the environment and the population. This information has major implications for assessing volcanic risk. Indeed, the sudden growth of the eruptive column during the course of the eruption may cause an increase in the particle size and thickness of the pyroclastic deposits (lapilli) accumulating on the ground and on the roofs, with a major impact on roof collapse, rail networks, etc., as well as, particularly in distal areas, an increase in the area exposed to ash fall, with potentially severe repercussions on agricultural crops over wide areas and extensive loss of livestock as a consequence of fluorosis. Moreover, a large amount of ash dispersed in the atmosphere can seriously disrupt air traffic.

1.1 The Vesuvius eruption in March 1944

The eruption in March 1944 was studied and described by various researchers at the time (e.g., Imbò 1945; 1949a, b, 1952, 1956; Parascandola 1945, 1948; Lazzari 1948; Casertano 1949; Scherillo 1949, 1953) who represent the point of reference for modern studies of the different eruptive phases, the deposition of eruptive products and the evolution of the feeding system (Scandone et al. 1986, 2008; Santacroce 1987; Cubellis and Luongo 1997; Pesce and Rolandi 1994; Villemant et al. 1993; Trigila and De Benedetti 1993; Marianelli et al. 1999, 2005; Fulignati et al. 2000, 2004; Del Moro et al. 2001; Morgan et al. 2004; Pappalardo et al. 2004; Lima et al. 2006, 2007; Chester et al. 2007; Ventura and Vilardo 2008; Vilardo and Ventura 2008; Cole and Scarpati 2010; Cubellis et al. 2013, 2014; Pappalardo et al. 2014).

The most exhaustive description of the eruption was that of the Director of the Vesuvius Observatory Giuseppe Imbò (Imbò 1949a, b) who, despite the severe events that affected the historic edifice of the Observatory during World War II, decided to intensify his observations of the volcano. The allied forces had taken over a large part of the edifice

despite Imbò's concerns: "… […] But I tried to express not only my personal regret but indeed of all scientists, not excluding the American volcanologists, for the abrupt interruption of the observations just before a possible violent paroxysm. The Italo-American lieutenant responded laconically with a smile: Volcanology is not necessary for war" (Imbò 1949b).

He followed all the stages of this eruption without leaving the edifice: "All other US servicemen… during the night before the beginning of the most violent paroxysm… had suddenly gone away and with them almost all the residents of the area. […] The Captain told me that a car was available for me if I wanted to go away immediately. I did not hesitate to say that my place was in the Observatory and that I would not abandon my position […]" (Imbò 1949b).

Imbò distinguished four main phases (Fig. 1), briefly reported below.

Besides supplementing our knowledge of the literature, since the sixtieth anniversary from the eruption eye-witness accounts have been collected (Cubellis and Marturano 2010) and put to use in this study, some of which agree with what is already known while others have added new elements to the phenomenon.

1.1.1 Phase I: effusive

"At 16:30 local time on March 18th, after a few hours of conduit obstruction, there was an abrupt reopening with the start of an intense effusive and explosive activity" […] (from the communiqué on the eruptive event of Giuseppe Imbò and reported by the daily newspaper "Risorgimento" March 25, 1944, Naples).

The eruption began in the afternoon of March 18, 1944, with the overflow of magma from the crater and the development of two main lava flows, one heading SSE, while the second flowed first northward and later, after reaching the border of the Somma caldera, was channeled westward.

Imbò climbed to the summit of the volcano, up to the crater, where he observed a mild strombolian activity accompanying lava flows. On 19th March, the effusive and explosive activity became more intense, and the lava flows, with a speed ranging from 50 to 300 m/h (Imbò 1949b), threatened the towns of San Sebastiano and Massa (Fig. 2), on the western slope of the volcano, that were invaded in the early hours of the 21st. Shortly before, the Allied authorities had organized the evacuation of about 7000 people living in these towns. In the afternoon of the same day the flows slowed and finally stopped on March 22nd; the SSE lava flows had reached an altitude of 350 m, while those that invaded San Sebastiano had stopped at an altitude of 140 m.
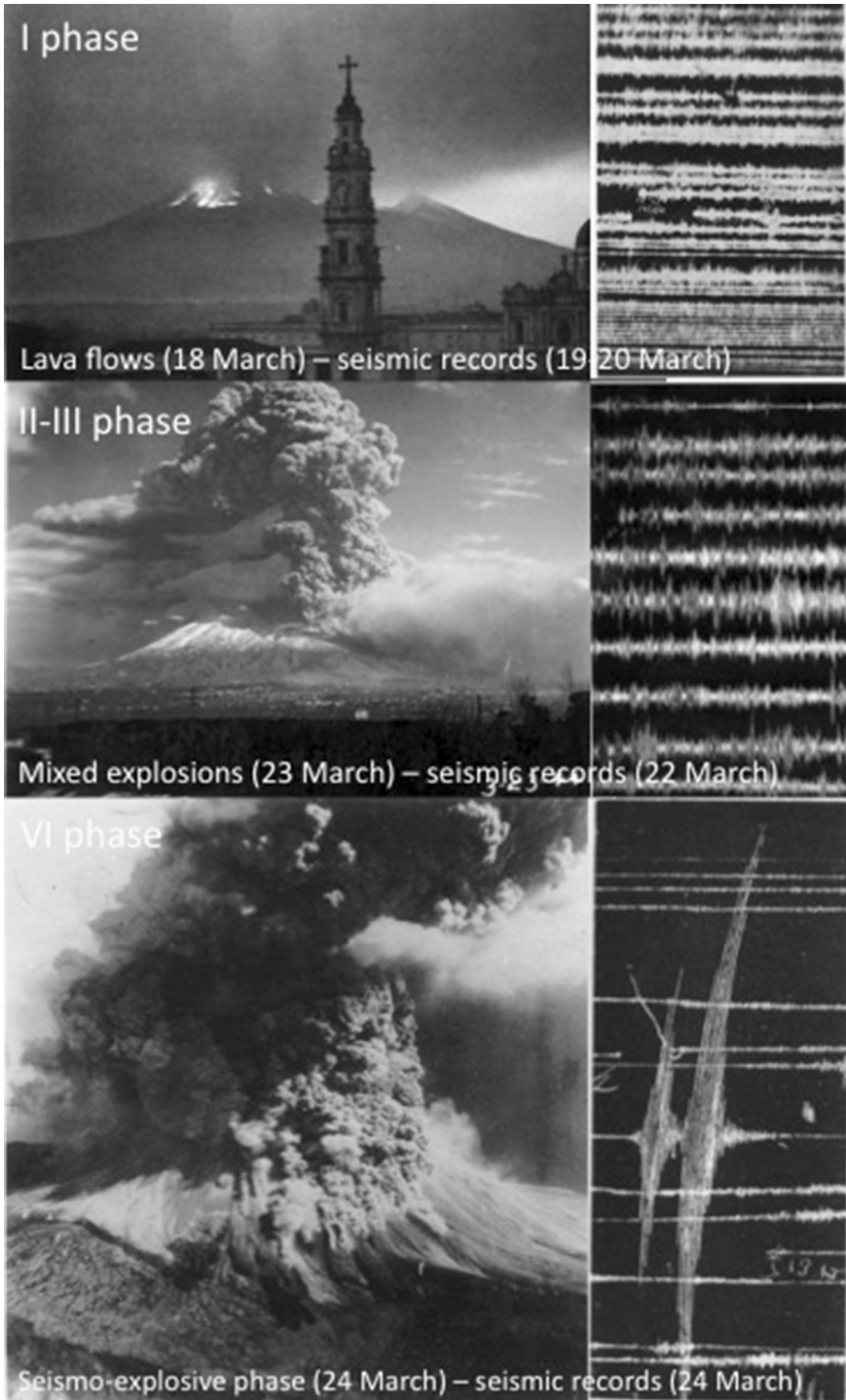
The following are quotes from eyewitnesses newly compiled by the authors:
From Portici (NA) (N 93.4 W, Fig. 2).

… a loud rumble and a continuous shaking propagated in the air…; a column of smoke rose rapidly in the sky; smoke first white, then gray. After a few days, you could see impressive lava flows that moved sometimes slowly, sometimes quickly […] The continuous tremors and bubbling like water in the pot … were especially impressive (Pasquale Migliaccio, Naples 2011).

From Naples (N 75.3 W, Fig. 2).

"… in the afternoon of March 18th, the windows jingled and it felt like a storm, but instead from the road we heard 'it is the Mountain.' We lived in Piazza del Gesù.

I phase

Lava flows (18 March) – seismic records (19-20 March)

II-III phase

Mixed explosions (23 March) – seismic records (22 March)

VI phase

Seismo-explosive phase (24 March) – seismic records (24 March)

◄ **Fig. 1** Eruptive and seismic activity during the different phases of the Vesuvius 1944 eruption. Seismograms were registered by the Omori-Alfani-Malladra (O.A.M.) seismometer that in 1944 was operating at the Vesuvius Observatory; each line corresponds to 1 h (the represented segments correspond to 11 min for phases I and II–III and to 3 min for phase IV. Photographs come from the archive of Vesuvius Observatory
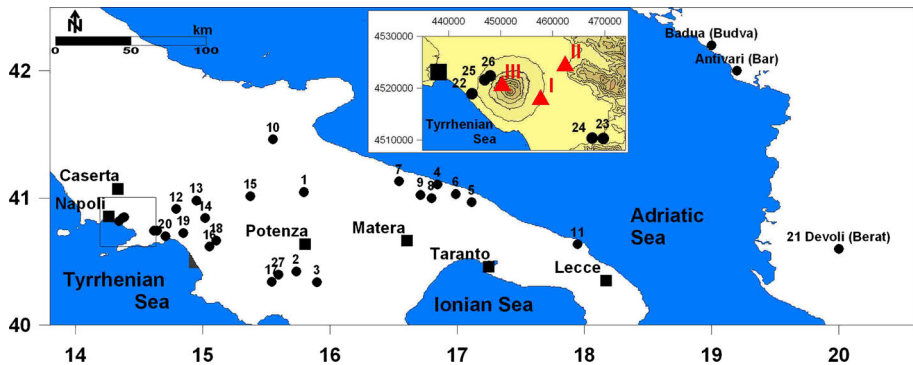

Fig. 2 The map shows the locations of the studied outcrops (red triangles: I Terzigno, II Palma Campania, III Vesuvius) and of the sites of ash accumulation (black dots) and/or locations of stories reported by eyewitness accounts. *1* Lavello (PZ), *2* Marsico Nuovo (PZ), *3* Viggiano (PZ), *4* Bari, 5. Conversano (Ba), *6* Noi Cattaro (Ba), *7* Terlizzi (Ba), *8* Sannicandro (Ba), *9* Binetto (Ba), *10* Foggia, *11* Brindisi, *12*. Avellino, *13* Lapio (AV), *14* Montella (AV), *15* Bisaccia (AV), *16* Eboli (Sa), *17* Monte San Giacomo (Sa), *18* Campagna(Sa), *19* Castiglione dei Genovesi (Sa), *20* Cava dei Tirreni (Sa), *21* Devoli (Albania), *22* Portici, *23* Nocera, *24* Pagani, *25* San Sebastiano. *26* Massa di Somma, *27* Sala Consilina (Sa)

Then the situation became bad on the 19th and the following days […]. (Roberto De Simone, Naples 2013).

1.1.2 Phase II: lava fountains

This phase began approximately at 17:00 local time on March 21st with an intense explosive activity characterized by eight "lava fountains." The volcanic fragments, falling on the summit of the volcano, formed a "pseudo-flow" (according Imbò 1949a) that appeared in the darkness of the night as "a black mass with red hot spots." Following the description of Imbò (1949a), the first fountain lasted less than 1 h (fountain I: between 17.15 and 17.45), with peak activity in the first 15 min, followed by seven other fountains of variable duration (fountain II: 20:10–20:30, fountain III: 22:00–22:25, fountain IV: 01:40–02:10 (22 March), fountain V: 03:45–04:03, fountain VI: 05:35–06:15, fountain VII: 0630–07:05), while the last one lasted over 5 h (fountain VIII: 7:30–12:30 March 22). But this, rather than a single fountain, were a "succession of fountains separate by maximum and minimum activity."

During the final phase of each fountain, an acoustic wave accompanied by a light arc was observed from the historical Vesuvian Observatory. This is likely the well-known phenomenon of a propagating shock wave, in which the temperature drop induced by rarefaction causes water vapor to condense into a visible arc.

Products associated with this explosive phase reached heights of up to approximately 4 km and, transported eastward by the wind, covered the towns around Vesuvius and the Agro Nocerino-Sarnese area, at distances of 15–20 km.

1.1.3 Phase III: mixed explosions

The end of the lava-fountain phase and the beginning of a new stage, called "phase of the mixed explosions," occurred shortly after noon on 22nd March. The volcanic cloud reached a height of over 5000 m above the crater, with the emission of black ash associated with the expulsion of "explosive" bombs (according Imbò 1949a) and "electrical discharges." Moreover, the partial collapse of the eruptive column generated small pyroclastic density currents sweeping at high speed (2–3 km/min) along the flanks of the Great Cone of Vesuvius down to its base. In this phase another important type of activity is the avalanching of the hot material accumulated on the cone as recognized by some authors (Hazlett et al. 1991; Chester et al. 2007). After a 3-h break in explosive and seismic activity, the second part of the mixed explosions began at 21:00 h of the same day with the emission of dark ash clouds from two contiguous vents and continued until the morning of 23rd March. This represented the climax of the eruption. Indeed, the column reached its maximum altitude above the crater and transported large quantities of ash that reached great distances from the vent. During the night of the 22nd and the morning of 23rd March at the oil field of Devoli (today Berat) in Albania (470 km from Vesuvius), a thin ash layer was deposited (Lazzari 1948).

During this phase of the eruption, 24 people died due to roof collapses caused by the accumulation of ash: twelve at Nocera, nine at Pagani and three at Terzigno (Fig. 2).

The following are quotes from eyewitnesses newly compiled by the authors:

From Naples (N 75.3 W, Fig. 2).

… I remember … it was about noon … we noticed a plume that was rising from Vesuvius and a dark cloud was expanding into the sky, a strange gray; it was very high. (Federico de Pandis, Riardo - CE, 2013).

On March 22nd, […] I remember the cloud of Mount Vesuvius was impressive: three times higher [about 4 km] than the volcano (Roberto De Simone, Naples 2013).

From what was then Yugoslavia (Fig. 2).

In March 1944 in Montenegro, Antivari (N 74.3 E), Porto Teodo and Budua (N 71.7 E), there was talk of ash falls from the Vesuvius eruption, and news about the event came from Radio Fante (Domenico Obrizzo, Naples, 2013).

From Devoli, Albania (N 91.6 E, Fig. 2).

On the night between 22nd and 23rd March, 1944, for an unspecified hour, at the AIPA oil shipyard in Devoli, Albania, a thin dark ash layer was deposited, I collected a sample thinking that it could be interesting to analyze (Lazzari 1948).

1.1.4 Phase IV: seismo-explosive

At about 12:00 noon on 23rd March, the explosions became discontinuous and the ash cloud reached altitudes not exceeding 2 km above the crater. Strong seismic activity was associated with the most intense explosive stages, while small pyroclastic density currents and landslides along the flanks of the Great Cone and electrical discharges in the atmosphere also characterized this phase of the eruption.

On the morning of 24th March, the eruptive activity had diminished and continued with less intensity until April 7th, when the crater was completely obstructed, giving rise to the current closed-conduit period of the volcano. This phase has been correlated to obstruction of the conduit and/or increase in magma viscosity.

1.2 Sampling and analytical methods

We examined representative samples of the deposits in order to study the chemical evolution of the eruption. The samples were collected from three stratigraphic sections located at different distances from the volcano: on the volcano's slopes (lava samples, phase I), at Terzigno (6 km ESE from the Vesuvius) (scoria samples from phases II and III), and at Palma Campania (12 km ENE from the Vesuvius) (scoria samples from both phases III and IV), as well as one ash sample, representing an extreme distal facies, collected at the time of the eruption in Albania (at 470 km E of Vesuvius, Fig. 2) by the geologist Antonio Lazzari (2013, 2014) who was there for oil exploration.

At Terzigno the sampled stratigraphic section is composed of a basal fallout deposit, 20–25 cm thick formed essentially of juvenile well-vesiculated scoria fragments ($Md\varphi = -3$, $\sigma\phi = 1$) (phase II). It is overlain by a 50-cm-thick, finer lapilli deposit composed of both lithic clasts and dense scoria fragments (phase III) with a mean size of $Md\varphi = -2$, $\sigma\phi = 1$.

At Palma Campania the sampled stratigraphic section is composed of a thin scoria layer overlain by an ash-rich deposit (phase IV). The last is a massive, 20 cm thick, well-sorted $\sigma\phi = 1$–1.15 (clasts size between 0 and 1ϕ) deposit.

1.2.1 Textural and geochemical analysis

Textural analyses were carried out on polished thin sections of epoxy-impregnated grains using a standard polarized light microscope. Analyses of major and volatile elements in groundmass glasses and mineral phases were performed with a JEOL-JXA-8200 electron microprobe (WD/ED combined micro analyzer) at the laboratories of the National Institute of Geophysics and Volcanology (Rome). Element concentrations were measured with a 10-μm beam at 15 keV, a beam current of 10 nA and a counting time of 10 s. For each analysis a defocused beam was used to minimize losses of alkalis and volatiles, which were counted first to avoid diffusion effects. We attempted to obtain at least ten analyses per sample. Data reduction was carried out using ZAF4/FLS software by Link Analytical. The analytical uncertainty was about 1 % for most elements. Results are reported in Table 1. The H_2O content of all analyzed glass was estimated by using the "volatile by difference" method based on EMPA analyses. The last technique has been widely used in petrology when, as in our case, the small size of the volcanic glass not allow the application of other methods (for example FTIR).

2 Results

2.1 Textural analysis

Lava and scoria samples are porphyritic with euhedral phenocrysts consisting chiefly of olivine (<1 %), plagioclase (5 %), diopside (10 %) and leucite (25 %), while garnet (<1 %), and phlogopite (<1 %), are very common accessory phases. The groundmass is rich in microlites (up to 50 vol%) represented generally by abundant leucite, minor feldspar, pyroxene, amphibole, and mica. The distal ash sample is composed mainly of free minerals (70–80 %) and to a lesser extent of vesicular dark glass (20–30 %). The main mineral phases are clinopyroxene (30 %), leucite (20–30 %) and feldspar (20–30 %); less

Table 1 Representative electron microprobe analyses of phenocrysts and glass of rocks of the 1944 Vesuvius eruption

Eruptive phase	Phase I	Phase IV	Phase II	Phase III	Phase IV	Phase I	Phase II	Phase III
Location	Vesuvius	P. Campania	Terzigno	Albania	P. Campania	Vesuvius	Terzigno	Albania
Samples	Lava	Pumice	Scoria	Ash	Pumice	Lava	Scoria	Ash
Phenocrysts	Leucite	cpx	Leucite	Leucite	Leucite	cpx	cpx	cpx
SiO_2	54.30	48.68	54.91	55.36	53.70	47.74	49.40	48.73
TiO_2	0.06	1.17	0.17	0.08	0.06	1.22	0.78	1.12
Al_2O_3	–	5.13	–	23.10	22.90	6.34	4.07	5.84
FeO	0.30	6.17	0.29	0.37	0.23	7.27	5.31	7.34
MnO	–	0.13	–	0.03	0.04	0.15	0.12	0.18
MgO	0.01	14.57	0.03	0.03	0.02	13.50	15.04	13.78
CaO	0.07	23.50	–	0.04	0.09	22.96	23.70	23.08
Na_2O	1.09	0.22	0.98	1.18	0.83	0.31	0.17	0.29
K_2O	19.45	0.01	19.93	19.56	20.25	0.01	0.01	0.02
P_2O_5	0.05	0.04	–	0.03	0.02	–	–	0.02

Eruptive phase	Phase I	Phase II	Phase III	Phase VI	Phase I	Phase II
Location	Vesuvius	Terzigno	Albania	P. Campania	Vesuvius	Terzigno
Samples	Lava	Scoria	Ash	Pumice	Lava	Scoria
Phenocrysts	Plagioclase	Plagioclase	Plagioclase	Plagioclase	Olivine	Olivine
SiO_2	45.27	48.03	50.16	47.28	37.58	36.92
TiO_2	0.04	0.04	0.04	0.03	0.13	0.02
Al_2O_3	33.95	31.03	30.50	33.08	0.03	0.05
FeO	0.64	0.62	0.59	0.50	25.27	25.71
MnO	0.01	0.02	0.03	0.01	0.55	0.67
MgO	0.07	0.05	0.08	0.06	37.79	35.82
CaO	16.82	14.53	13.98	16.09	0.57	0.49
Na_2O	1.42	2.88	3.07	1.97	–	0.03
K_2O	0.28	0.19	0.54	0.31	–	–
P_2O_5	0.03	0.02	0.02	0.02	0.10	–

Table 1 continued

Eruptive phase Location Samples Phenocrysts	Phase III Albania Ash Olivine	Phase IV P. Campania Pumice Olivine	Phase I Vesuvius Lava Glass	Phase II Terzigno Scoria Glass	Phase III Albania Ash Glass	phase VI P. Campania Pumice Glass
SiO_2	36.91	40.68	48.78	48.25	46.26	46.10
TiO_2	0.08	0.01	0.87	0.95	1.19	1.36
Al_2O_3	0.06	0.04	18.02	19.22	17.56	17.27
FeO	25.90	9.48	9.72	8.09	10.01	10.02
MnO	0.56	0.22	0.26	0.20	0.21	0.20
MgO	37.42	51.09	2.69	3.12	3.92	4.09
CaO	0.51	0.31	8.78	9.22	8.74	9.86
Na_2O	0.02	–	6.38	3.16	4.30	3.64
K_2O	0.01	–	2.76	5.51	4.55	4.85
P_2O_5	0.08	0.02	1.17	1.02	1.25	1.25
F	–	–	0.53	0.26	0.30	–
Cl	–	–	0.81	0.37	0.38	0.59

The reported analyses are the mean values of those published in Pappalardo et al. (2014)

abundant olivine (5 %), magnetite (5 %), apatite (<1 %), titanite (<1 %) and garnet (<1 %), in accordance with what was reported also by Lazzari (1948). Similar composition has described by Scherillo (1953) for volcanic ash deposited at Brindisi during the same eruptive phase.

Ash is constituted by tabular or elongated clasts (aspect ratio = ~1.5 modal value; circularity = ~0.7 modal value), with moderate roundness (roundness = ~0.7 modal value) and size ranging between about 20 and 350 μm (Fig. 3).
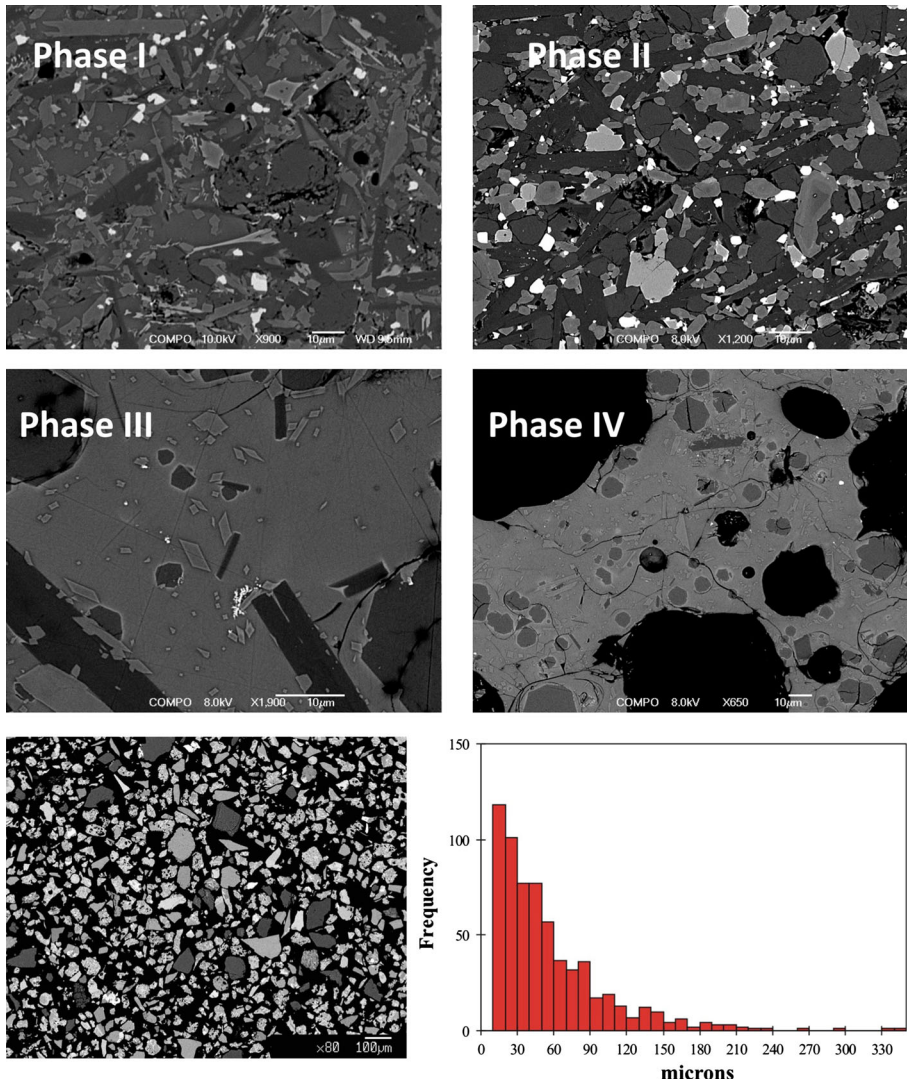

Fig. 3 Back-scattered electron (BSE) images of groundmass textural features in samples from the different stages of the Vesuvius 1944 eruption and of the volcanic ash collected at Devoli in Albania (470 km from Vesuvius) (*lower-left*) and histogram of the clast size (*lower-right*). The dimension of the clasts is between 20 and 350 μm, with a prevalence of smaller clasts (20 and 30 μm)
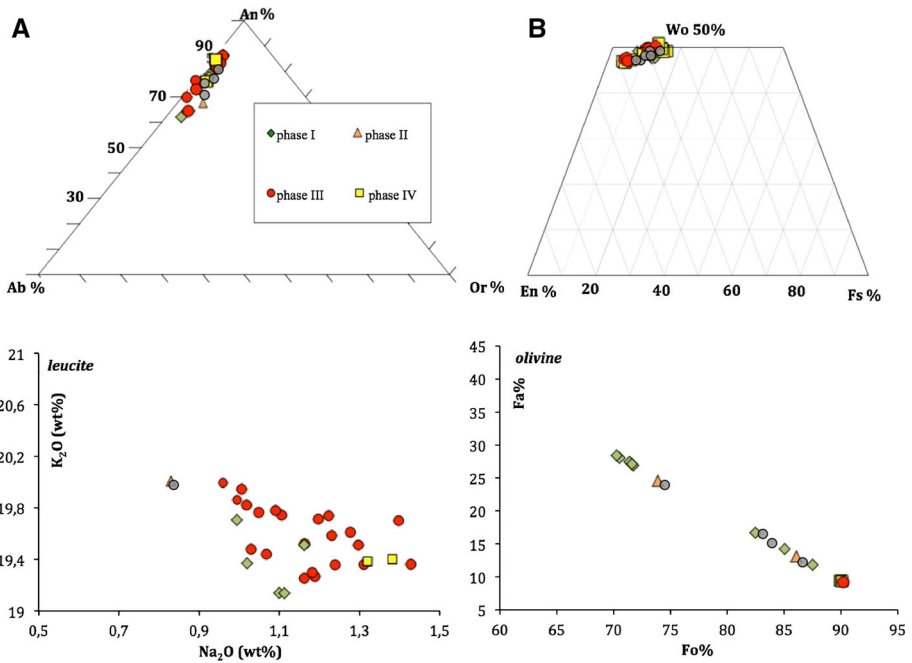
Fig. 4 Chemical composition of the main mineral phases. **a** Ab–An–Or plot for feldspars; **b** En–Wo–Fs plot for clinopyroxenes; **c** K_2O versus Na_2O in leucite crystals and **d** Fo % versus Fa % in olivine. The figure shows that the chemical composition of phenocrysts is similar for all the studied products (lavas, scoria and ash) emitted during the different phases of the eruption. *Gray symbols* data from literature (Marianelli et al. 1999)
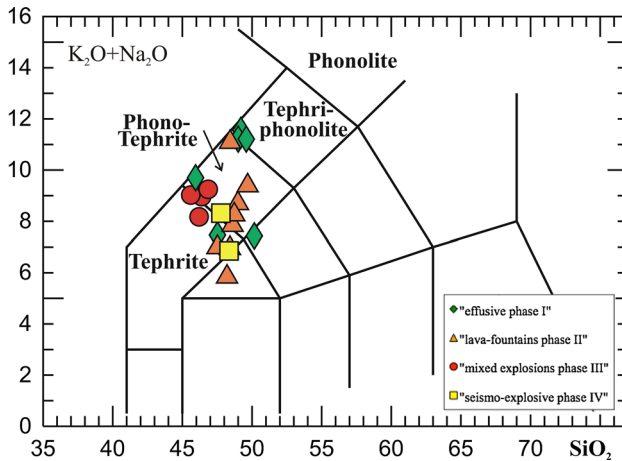

Fig. 5 Total Alkali Silica classification diagram (Le Bas et al. 1986). The groundmass glass has a composition ranging from tephrite to phonotephrite

In spite of the quite uniform phenocrysts content, the analyzed volcanic samples show different textural characteristics in microlites. The last feature has been deeply explored by Pappalardo et al. (2014) and briefly reported here. In particular, microlite crystals in lava

Fig. 6 Harker diagrams of major element compositions in whole rocks [*open symbols* data from Marianelli ▶ et al. (1999)] and volcanic glass (*closed symbols* data from this paper) emitted during the 1944 eruption. Symbols are as in Fig. 5. The regular patterns of major element concentrations versus the index of magmatic differentiation (MgO) indicate a gradual and continuous process of crystallization in the magmatic system. See text for further explanations

(effusive phase I) and subordinately scoria (lava-fountains phase II) samples are composed of larger prismatic plagioclase (60–80 μm, 3.5–4ϕ) associated with smaller blocky clinopyroxene (30 μm, 5ϕ). While pumice and ash (sustained-column III phase and vulcanian IV phase), contain microlites represented by sparse smaller acicular clinopyroxene and in minor amount plagioclase (15–10 μm, 6ϕ), Fig. 3.

2.2 Mineral chemistry and glass composition

2.2.1 Feldspar

The feldspar compositions are reported in an albite–orthoclase–anorthite diagram in Fig. 4. Our data indicate that lavas, scoria and ash samples are characterized by plagioclase of bytownitic-labradoritic (An_{84-64}) composition.

2.2.2 Pyroxene

The composition of pyroxene phenocrysts are shown in the Enstatite–Ferrosalite–Wollastonite diagram (Fig. 4; Morimoto 1988). The analyzed pyroxenes fall in the diopside field for lava, scoria and ash samples and show a general trend toward Fe-rich composition (Fs_4–Fs_{14}).

2.2.3 Leucite and olivine

The phenocrysts of leucite show fairly homogeneous composition ($K_2O = 19.2$–19.8 wt%). The olivine crystals have a content of forsterite of Fo_{71-90} (Fig. 4). In general, the chemical composition of phenocrysts is similar for all the studied products (lava, scoria and ash) emitted during the different phases of the eruption.

2.2.4 Volcanic glass

The groundmass glass has a composition ranging from tephrite to phonotephrite (Fig. 5) in the classification diagram of Le Bas et al. (1986). In Fig. 6 the most representative variation diagrams are shown for major elements (Harker diagrams) as a function of MgO, used as a magmatic differentiation index. In the Harker diagrams the total composition of the whole rocks (glass + crystals) is always less differentiated than that of the corresponding volcanic glass. With the decrease in MgO concentration, major elements describe regular patterns without compositional hiatus. In particular, we observe an increment of SiO_2 (45–51 wt%), Al_2O_3 (13–22 wt%), Na_2O (from 1 to 8 wt%), MnO (from 0.15 to 0.35), and a decrease in FeO * tot (from 11 to 7 %), CaO (14–6 %), while TiO_2 (from 1 to 1.4 %) and P_2O_5 (from 0.6 to 1.4) slightly increase except for lava and scoria glass groundmass possibly due to their nearly complete microlite crystallization. By contrast, K_2O increases in less differentiated rocks (MgO between 8 and 5 wt%), while it decreases in the samples with a higher degree of evolution (MgO between 5 and 2 wt%).
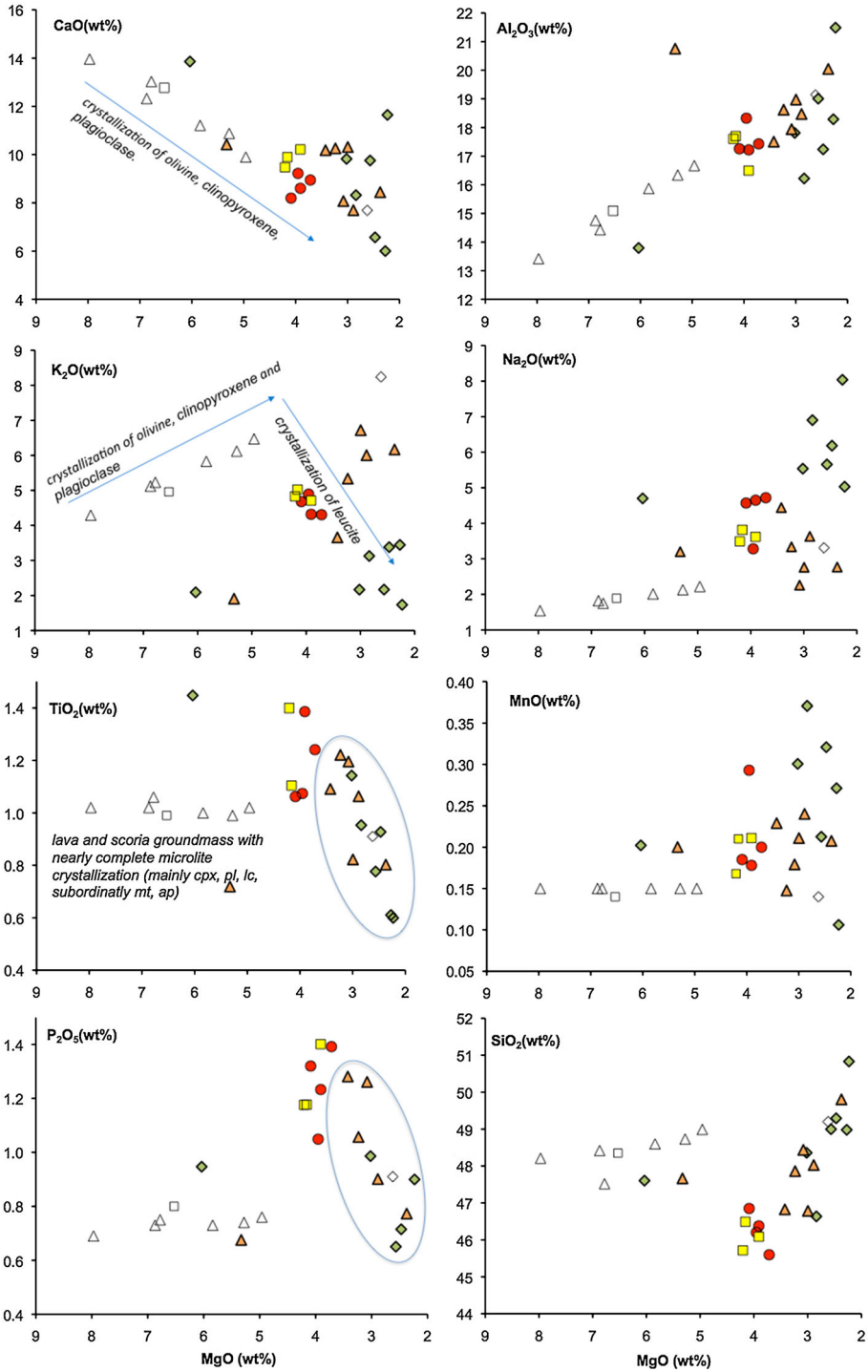
These compositional variations can be attributed to the fractional crystallization of phenocryst phases observed in the rocks. In particular, the decrease in MgO, FeO * tot and CaO is consistent with the predominance of the fractionation of mafic minerals (rich in Mg and Fe, such as olivine and clinopyroxene) and calcic plagioclase, while the roughly constant concentrations of TiO_2 and P_2O_5 indicate the crystallization of minerals rich in Ti and P (biotite, magnetite, apatite, spinel) as accessory phases. Furthermore, the reversal of the slope shown by K_2O content (Fig. 6) which, from initial enrichment, decreases in samples less rich in MgO (<5 %) may indicate a late crystallization of leucite, in whose crystal lattice K is concentrated which is consequently subtracted in the more evolved liquid. The last result is in agreement with experimental data indicating that the crystallization of leucite in Vesuvius magmas occurred at the pressure <100 MPa and under rapid growth rate (Shea et al. 2009).

2.3 Magma evolution and conduit dynamics

To constrain the conditions of temperature and pressure at which the different mineral phases are crystallized, we used the chemical compositions of minerals and glass obtained by the electron microprobe in the thermodynamic calculations (Fig. 7) based on the minimization of Gibbs free energy (MELTS CODE, Ghiorso and Sack 1995) performed by Pappalardo and Mastrolorenzo (2010) on Vesuvius tephritic rocks. Furthermore, the pressure values obtained by using the concentrations of volatile phases (H_2O, Cl, F) measured in volcanic glasses (which represent the fractions of residual degassed liquid in the conduit) were compared with those available in the literature (Marianelli et al. 1999; Fulignati et al. 2000) on melt inclusions (small drops of non-degassed magma) trapped in the crystals during their growth (Fig. 8), and on experimental studies (Pichavant et al. 2014).

Our results indicate that crystallization is carried out in two distinct phases under different conditions of pressure and temperature. In the first phase the less evolved magma cools ($T = 1150$–950 °C) in a crustal magma chamber at depths between 16 and 8 km (P between >400 and 300 Mpa), confirming the data on melt inclusions (Marianelli et al. 1999; Fulignati et al. 2000). The same phase crystallizes mainly olivine and pyroxene, and to a lesser extent plagioclase, magnetite and apatite (Fig. 8). A second crystallization phase occurs with lower pressure (<200 Mpa) and temperature (<950 °C), probably during the ascent of the magma in the volcanic conduit, in which the leucite crystallizes in equilibrium with the evolving magmatic liquid (Fig. 8). The obtained data agree with experimental results showing that the primitive Vesuvius trachybasalts crystallize Fo-rich olivine as the liquidus phase between 1150 and 1200 °C and from 300 to <200 MPa (Pichavant et al. 2014).

Information on the ascent rate of the magma in the volcanic conduit during the different phases of the eruption can be deduced from the volatile content measured in volcanic glass (Fig. 9), whose composition corresponds to that of the residual magma during degassing in the volcanic conduit. In particular, the low water contents (H_2O wt% ∼0.5–1.6) which characterize the samples of lava emitted during the effusive phase are compatible with a slow decompression of the magma in the volcanic conduit that favors volatile exsolution, bubble diffusive growth and coalescence (that controls magma permeability) and then removal of gas (including H_2O) from the liquid (near-equilibrium degassing path). In contrast, the highest water content (H_2O 1.5–3 wt%) in scoria and ash of the explosive phases of the eruption is indicative of more rapid rising in an unlocked volcanic conduit that prevents the diffusion of the gas phase, which remains dissolved in the melt until
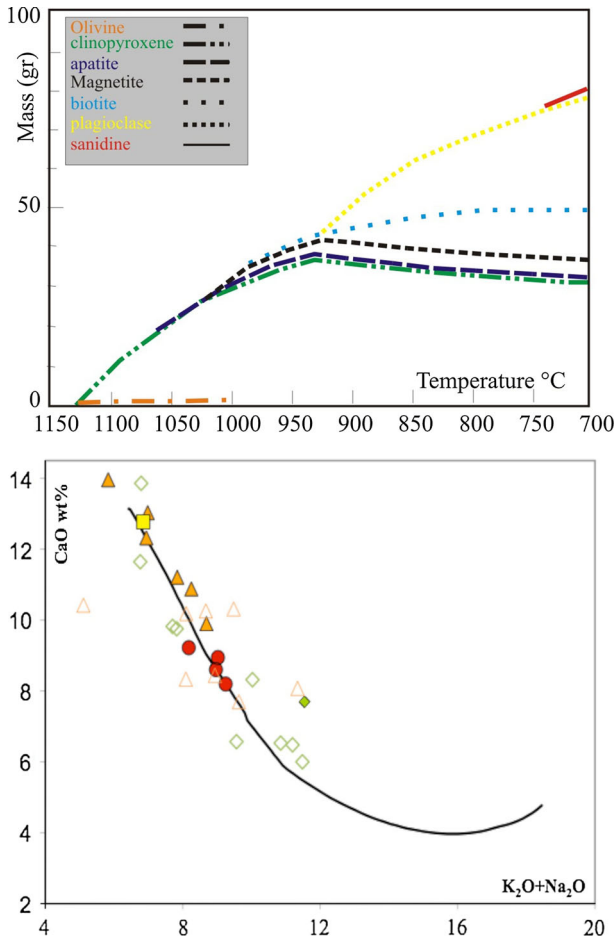
Fig. 7 Mineralogical assemblage (*top*) and magma (*bottom*) composition during the process of crystallization simulated using the program Melts following the procedure used by Pappalardo and Mastrolorenzo (2010). *Symbols* as in Fig. 6

explosive fragmentation occurs (disequilibrium degassing path). Actually, during decompression experiments both degassing paths were observed in Vesuvius magma (Marziano et al. 2007); particularly in the case of higher decompression rate, magma ascent is characterized by high water over- saturations under disequilibrium condition, while for slower ascent rates degassing of the melt by diffusive bubbles growth prevails, thus sensibly reducing the water over-saturation in the melt.

Different degassing mechanism during rising in volcanic conduit is suggested also by the trend of Cl and F contents in function of CaO wt%, chosen as index of differentiation (Fig. 9b, c). The figures show that F and Cl contents increase in lavas with the degree of differentiation of rocks while remain constant in ash and scoria. Signorelli and Carroll (2000) have shown that Cl increases within melts, saturated with both a H_2O vapor phase and a Cl-rich brine, as pressure decreases. The lavas of the phase I follow this Cl solubility model, corroborating the hypothesis of an initial slow ascending magma, while scoria and
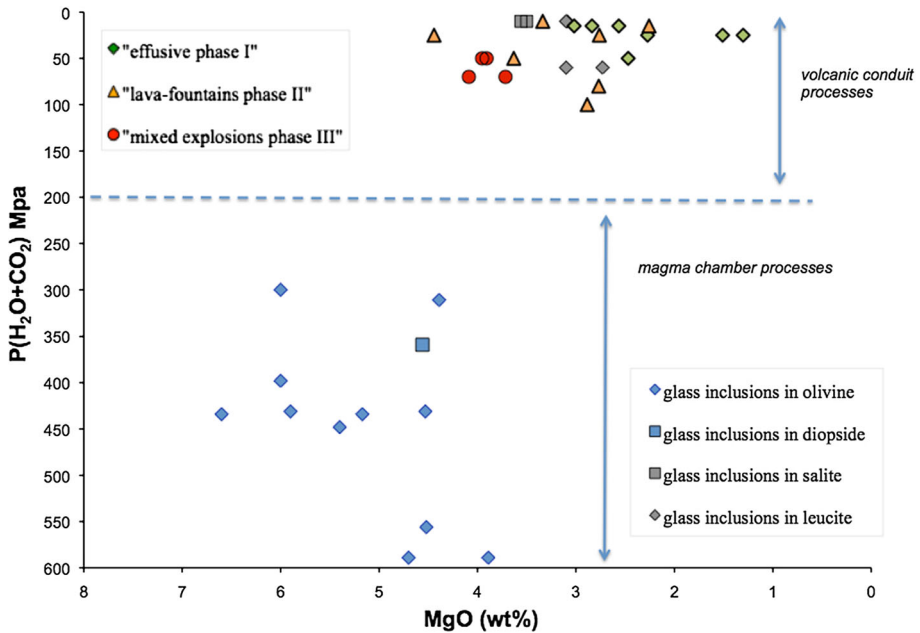
Fig. 8 Composition of glass inclusions (magma chamber processes) trapped in the main mineral phases of the 1944 eruption (data: Marianelli et al. 1999; Fulignati et al. 2004) compared with the composition of volcanic glass (volcanic conduit processes). For volcanic glass analyzed in this study, the values of pressure are calculated on the basis of water content measured by "difference method." See text for further details

ash of the following phases show a constant Cl concentration, indicating a fast ascent rate which prevents fluid/melt Cl exchange.

2.4 Estimation of the maximum height of the eruptive column during the paroxysmal phase

Historical chronicles report that during the paroxysmal phase of the eruption, between March 22nd and 23rd, the volcanic ash reached great distances from the vent, as far as Devoli in Albania (470 km from Mount Vesuvius), and that the eruptive column reached 5000 m in altitude. However, this altitude estimate is not compatible with the long distance reached by the ash. Indeed, Chester et al. (2007) assumed that the cloudiness did not allow the witnesses to accurately determine the maximum height reached by the column. To test the hypothesis of Chester, we consulted the archives of the weather station of the Geophysics Institute of the University of Naples located at the city center. Data show that the sky on March 22nd 1944 had a cloud cover of 3/10 in the early afternoon (14:00), while in the evening (19:00) there was total cover (10/10), which lasted throughout the following day, thus not allowing observation of the eruptive column in its full development. Therefore, to constrain the maximum height reached by the eruptive column during the paroxysmal phase of the eruption, we adopted a numerical model of volcanic ash dispersion into the atmosphere (Mastrolorenzo et al. 2008), using both the dynamic parameters (initial velocity, erupted mass, ash density and size) of the eruption phase (Scandone et al. 1986; Pfeiffer et al. 2005; Macedonio et al. 2008) and the measured wind speed in
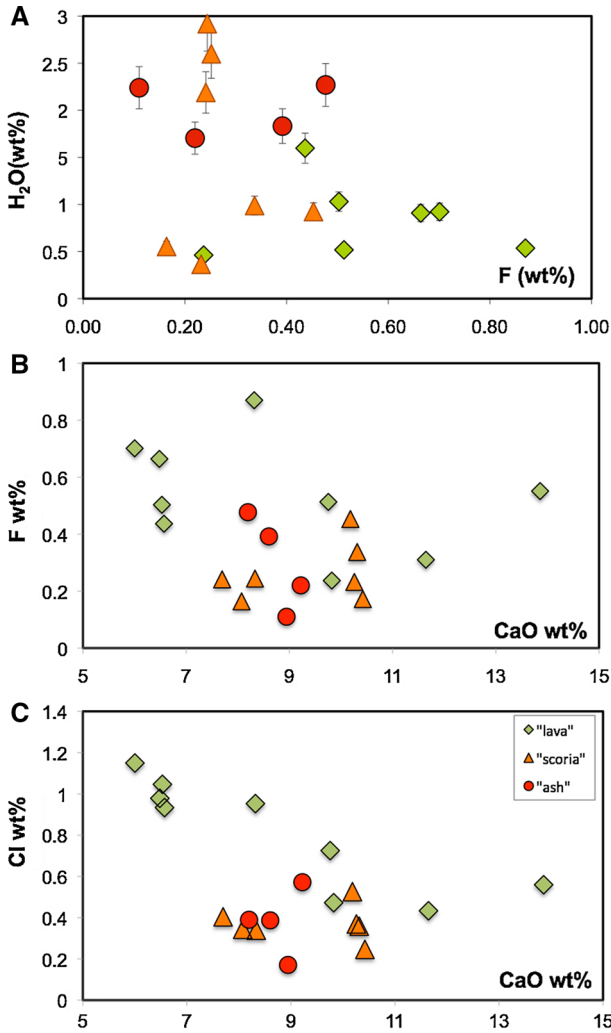
Fig. 9 **a** Water content versus F, **b** CaO versus F and **c** CaO versus Cl in the volcanic glass of the different phases of the eruption. The lava emitted during the first effusive phase shows the lowest water content, compatible with a slow ascent of the magma in the conduit, which favors exsolution and the removal of volatiles including mainly H_2O (equilibrium degassing); by contrast, glass samples of explosive phases show higher water content indicating faster rising, hindering the exsolution and escape of magmatic gas (disequilibrium degassing)

March 1944 at different altitudes up to 12,000 m (Fig. 10 database of NOAA's National Geophysical Data Center, http://www.ngdc.noaa.gov/).

It is possible that the volcanic column has acted as a "weak" plume at least in the second phase of the eruption as suggested by photos taken at that time showing a few km high plume following bent-over trajectories strongly controlled by the wind strength and direction. While it possibly has switched to "strong" plume during the paroxysm of the third phase (for which unfortunately no photos are available) when it reached its maximum height and transported ash until Albania and Yugoslavia. In our model we have considered
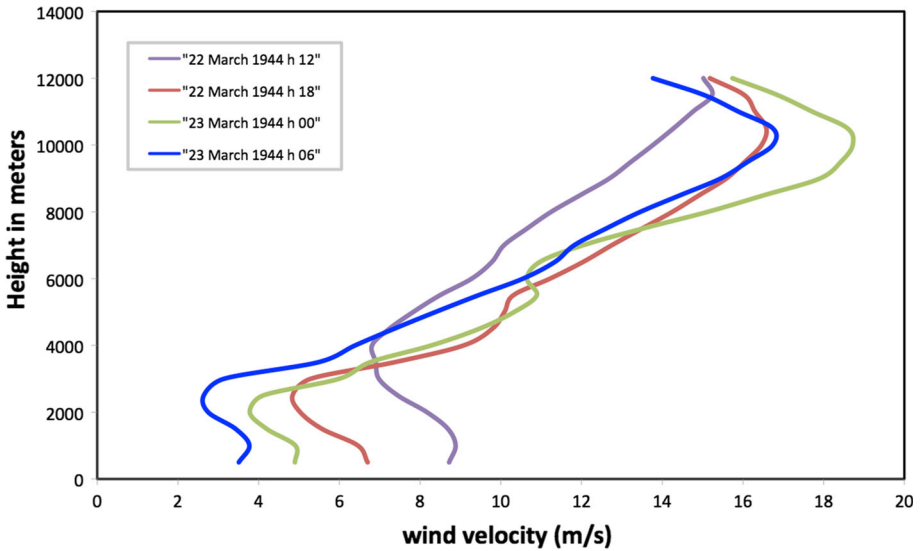
Fig. 10 Wind speed in the direction of the parallel (to the east), measured at different altitudes on 22 and 23 March 1944, during the paroxysmal phase of the eruption in which the arrival of volcanic ash was documented in Albania

exclusively this second behavior to calculate the maximum height of the column necessary to justify the falling of ash, so far from the volcano during the third eruptive phase.

The results of the simulations, shown in Fig. 11, indicate that the eruptive column reached a height of around 10 km to justify the accumulation of a thin layer (about 1 mm) of ash in Albania approximately 470 km away from Mount Vesuvius. The data obtained are in agreement with those calculated by other authors from the analysis of lithic and scoria isopleths (Cole and Scarpati 2010). On the basis of the obtained height of the column and of the data on wind speed at different altitude (Fig. 10), it is possible to calculate that the ash, carried by high-altitude winds toward east with a mean speed between 50 and 70 km/h, has to have travelled for 7–9 h before reaching the Albania between the night of the 22nd and the morning of 23rd March as reported by Lazzari (1948).

Figure 11 also shows the thicknesses of the accumulated ash in the third eruptive stage along the dispersion axis, as testified by numerous witness reports collected in the last 10 years in a wide area (Cubellis and Marturano 2010, Cubellis et al. 2013), according to which the ash fall reached considerable distances from the volcano (Table 2).

Data in Fig. 11 indicate that, for distances below 100 km from Vesuvius, ash thicknesses are consistent with a cloud height of about 5 km, while those accumulating at greater distances reflect a column height of between 8 and 10 km. This apparent bimodality could be explained by a rapid change in eruptive regime during column development. According to Pappalardo et al. (2014), during phase III the partial collapse of the deeper parts of the plumbing system caused a pressure drop at the top of the underlying chamber and then the rapid extrusion of a larger volume of magma in a short time. This process could explain the rapid increase in the height of the eruptive column during the paroxysmal phase and hence the bimodal distribution, observed in Fig. 11, relative to the thickness of ash accumulated during the phase III, due to the discontinuous growth of the
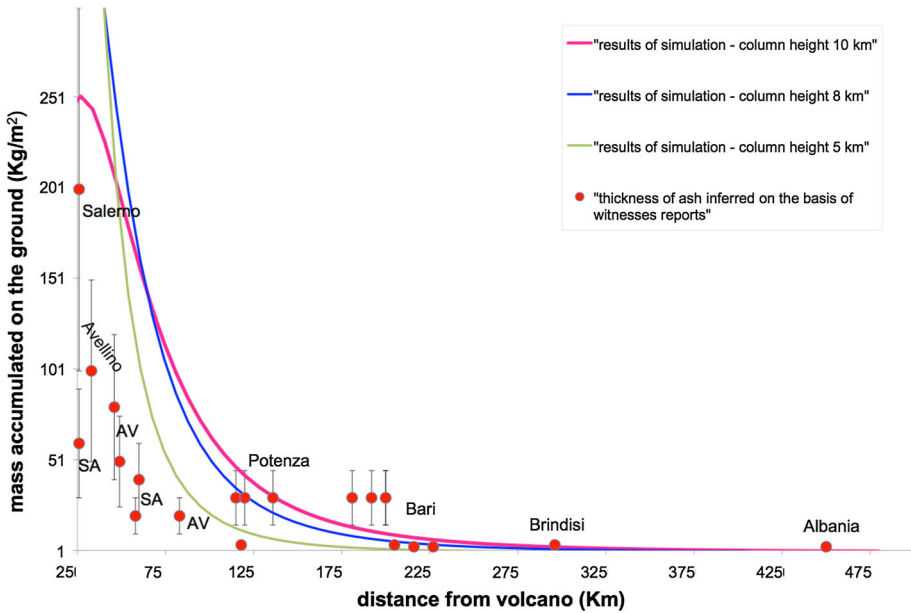
Fig. 11 Numerical simulation of dispersion of volcanic ash in the atmosphere carried out using the dynamic parameters of the 1944 eruption (initial velocity $= 200$ m/s, erupted mass $= 0.4 \times 10^{12}$ kg, average density $= 1000$ kg/m^3 and average size of the ash $\phi = 1.5$) and the wind speed measured in March 1944. The figure shows that, for a column height of 5 km, the ash reaches about 200 km away from the volcano; for a height of 8 km, ash arrives at 300 km away, while for an eruptive column higher than 10 km, the distance exceeds 400 km. Thickness of ash resulting from direct accounts is also reported. For distances below 100 km, the observed thicknesses are consistent with a cloud height of about 5 km, while the thicknesses accumulating at greater distances reflect a column height between 8 and 10 km

eruptive column as well as in the proximal area (sections located <5 km from the crater) the well-developed reverse to normal grading, as described by Cole and Scarpati (2010).

2.5 Impact on the environment and people

The real impact of the last Vesuvius eruption on the environment and people is still now not well evaluated, possibly due to the extensive destruction of Neapolitan area and the death of tens of thousands of civilians related to the World War II, as recently speculated on the basis of new historical reconstructions (Cole and Scarpati 2010; Romano 2011; Cubellis et al. 2013, 2014; Cubellis and Marturano 2014) and confirmed by the eyewitness accounts of the eruption.

The following are quotes from eyewitnesses recently compiled by the authors:
From Naples:

> Remembering after over 70 years an exceptional yet dramatic event like the 1944 eruption of Vesuvius arouses in me a strange emotion … […] We were living in difficult times, the war with all its horrors had overrun Naples, […] we were still suffering from hunger and the consequences of the bombings … without forgetting the outbreak of epidemic typhus.

Table 2 Thickness of volcanic ash emplaced during the phase III

Location	Distance (km)	Reported thickness (mm)
1. Lavello (PZ)	118	2–5
2. Marsico Nuovo (PZ)	120	10–40
3. Viggiano (PZ)	136	10–40
4. Bari	205	2–5
5. Conversano (Ba)	227	2–3
6. Noi Cattaro (Ba)	216	2–3
7. Terlizzi (Ba)	181	30
8. Sannicandro (Ba)	200	10–40
8. Sannicandro (Ba)	200	10–40
9. Binetto (Ba)	192	10–40
10. Foggia	115	10–40
11. Brindisi	296	2–5
12. Avellino	33	100
13. Lapio (Av)	46	80
14. Montella (Av)	49	50
15. Bisaccia (AV)	83	20
16. Eboli (Sa)	58	20
17. Monte San Giacomo (Sa)	107	20
18. Campagna(Sa)	60	30–50
19. Castiglione dei Genovesi (Sa)	26	30–80
20. Cava dei Tirreni (Sa)	26	200
21. Devoli (Albania)	450	1

[…] news came that there were 'several dead'. But even this news, dramatic though it was, I don't remember especially scaring me. … we were perhaps used to hearing about deaths due to bombings or in action on the various frontlines. (Ugo Foà, Rome, 2015)

Our new data on both the development of the eruptive column (previous paragraph) and the new witness reports allowed to add information on the effects of the eruption on the environment and human activities. Particularly, our calculation of the maximum height of the eruptive column and the consequent dispersion of ash over a wide area can justify the extensive loss of livestock documented by the new eyewitness accounts, also at great distances from the volcano (not less than 120 km). In fact the death of sheep, lamented by most of the survivors, was probably the consequence of fluoride poisoning (fluorosis) procured by the intake of grass from pastures covered with ash, in analogy with what has been observed for other historical and recent eruptions in other parts of the world. Particularly, in 1693, the first fluorine intoxication of animals due to a volcanic eruption was reported from Iceland after eruption of Hekla volcano (Thorarinsson 1979). A similar behavior was observed at Hekla again in the 1970 (Georgsson and Pétursson 1972). In 1783, ashfall and gases from Lakagigar volcano, once again on Iceland, caused the death of tens of thousands of sheep, cattle and horses (Cronin et al. 2003).
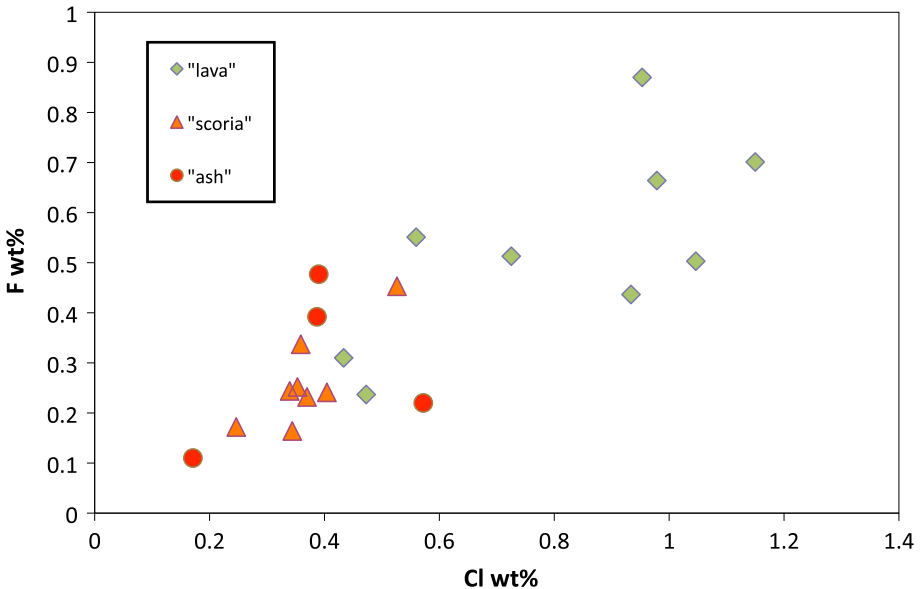
Fig. 12 F and Cl concentrations in lava, scoria and ash samples of the 1944 Vesuvius eruption

More recently, in 1988, about 10,000 farm animals were affected by fluoride-bearing ashes from the Lonquimay volcano eruption in Chile, killing more than 4000 head (goats, sheep, cattle and horses), while ashfall from Ruapehu volcano eruptions caused the death of thousands of sheep in 1995–1996 probably by fluorosis (Armienta et al. 2011).

To prove our hypothesis, we have measured the content of F in the volcanic products emitted during the course of the eruption, the obtained concentration actually is above the threshold of lethality for livestock. The amount of F in the lava, scoria and ash of the 1944 eruption is shown in Fig. 12. The amount considered lethal to grazing animals is at least 100 µg/g body weight (NRC, 1974) (4–5 g for animals weighing 40–50 kg), while values close to 50 µg/g seem to be tolerated by sheep and cattle. Fluoride concentrations of 2000 ppm (0.2 %) and Cl/F ratios similar to those reported in Fig. 12 of ash from explosive eruptions caused acute fluorosis and mortality in sheep during the eruption of the volcano Hekla in 1970 (Georgsson and Pétursson 1972). With these F concentrations, a layer of ash even one mm thickness is sufficient to cause the death of animals. In fact, following the reasoning of Dawson et al. (2010), we consider that the 1944 ash contains 2 g fluoride kg^{-1} ash (Fig. 12) with a density of 1 g/cm^3, a 1-mm deposit covering 1 m^2 would represent 1 kg of ash, equivalent to 10 tonnes ash ha^{-1}. A sheep eating 1.6 kg dry mass herbage day^{-1} on a pasture at 4000 kg dry mass herbage ha^{-1} (Dawson et al. 2010) would be eating the equivalent of 4 m^2 of herbage, and 4 kg volcanic ash (8 g fluoride), if all of the ash was deposited on the herbage. Under such circumstances, the sheep would receive fluoride at very high toxic levels.

The following are quotes from eyewitnesses recently compiled by the authors:
From Marsico Nuovo (PZ) (N 111.9 E, Fig. 2).

11 of 12 of them [goats] died after a few days of each other. The survivor, the only non-pregnant animal, lost considerable weight. Even the flocks of neighbors suffered more or less the same fate. (Raffaele Vignola, 2014).

From Sala Consilina (SA) (N 115.3 E) (Fig. 2).

[…] In the town (about 1700 inhabitants, 668 m a.s.l.) … it happened that grazing livestock died, mostly because they had eaten grass mixed with 'charcoal' (that was what the volcanic ash were called). With sheep, goats, lambs etc. a cow also died, again for the same reason. These animals all died with enormously bloated stomachs. (Italo Taccelli, Sala Consilina, SA, 2012).

Besides the loss of livestock also the number of casualties may be greater than known until now.

Reports of the Allied Military Government (Daily newspaper "Risorgimento" March 26th 1944 Naples) indicate that during the eruption 26 people died (12 at Nocera, 9 at Pagani, 3 at Terzigno) for the collapse of the roofs; also, two children from San Sebastiano and Massa di Somma died from the explosion of a tanker due to the passage of lava flows. The largest number of victims is due to the paroxysmal phase, as shown by numerous death certificates from the parishes of Nocera and Pagani. That said, the number of victims could have been even higher than officially reported at the time of the eruption. Indeed, because of the war some deaths went unreported.

The following are quotes from eyewitnesses newly compiled by the authors:
From Terzigno (NA) (N 104.7 E, Fig. 2).

[…] "The rain of this material [ash and lapilli] in the roads and on the roofs prevented normal traffic and threatened the stability of the dwellings.

This is why my brothers and my father started to clear the roof of our house on Via Roma. On the third day of the eruption, during the morning, my brothers were on the roof and my father, realising that it had begun to rain [ash and lapilli] once again, wanted to call them back. But while he was looking out of the front door, he was hit on the temple by a hot stone (a volcanic bomb) the size of a tennis ball and died on the spot.

The difficult moment and the poor state of the streets prevented the body being transported from our house to the cemetery". […] (Maria Rosaria Fabbrocini, Ottaviano, 2014).

3 Discussion

Our results allowed us to reconstruct the eruptive dynamic during the last Vesuvius eruption in March 1944. In particular, the chemical compositions of volcanic rocks indicate that the magmas feeding the four phases of the eruption have similar geochemical and petrological imprints, such that the transition to the paroxysmal phase of the eruption is not related to changes in magma pre-eruptive conditions but instead to rising processes in the volcanic conduit.

Thermodynamic calculations based on the chemical equilibrium between crystals and liquid indicate that magmatic differentiation took place in two stages of crystallization under different temperatures and pressure conditions. In a first phase of higher pressure, the cooling of less evolved magma in a crustal magma chamber (between 16 and 8 km depth) caused the crystallization mainly of olivine and diopside and to a lesser extent plagioclase, magnetite and apatite; while in the later lower pressure stage (depth < 8 km), probably associated with the ascent of magma in the volcanic conduit, crystallized mainly leucite in equilibrium with the evolving residual liquids. This

process of leucite syn-eruptive crystallization in the volcanic conduit, associated with a more rapid ascent of magma as suggested by our data on volatile concentrations in the melts, could explain the emission of magma richer in gas, and hence the sudden increase in the degree of explosiveness of the eruption in the intermediate stages (phases II and III), with the emission of a greater amount of ash. Other authors (Marianelli et al. 1999), on the basis of melt inclusions data, have recognized that the magmas feeding the eruption underwent differentiation at different pressures and suggested that the paroxysmal phase was fueled by the arrival of new, volatile rich, magma from the depth.

However, the increase of the ascent rate during the course of the eruption, has been recently documented by Pappalardo et al. (2014) trough the study of groundmass microlite textural variations (microlite number density MNDs and size distributions MSDs). Particularly, these authors have shown a progressively increase of the value of MNDs as well as of the slope of CSDs from lavas (MNDs = 11,673; slope = −30) and scorias (MNDs = 10,895–25,803; slope = −120), erupted, respectively, during the phase I and phase II, to pumices and ashes from the phase III and phase IV (MNDs = 40,000–35,000; slopes = from −175 to −608). These data allowed to demonstrate that decompression became gradually faster during the eruption, ranging from few days at the beginning of phase I up to few hours during the most violent paroxysm (phase III), with the development of a high eruptive column.

Historical chronicles report a height of the eruptive column during the paroxysm of about 5000 m. However, this value is hardly compatible with the high distance of ca. 500 km from the volcano that was reached by the volcanic ash. Possibly the presence of cloudiness on March 22–23rd 1944, did not allow the witnesses to accurately determine the maximum height reached by the column. In fact, our analysis of the data of the weather station of the Istituto di Geofisica of the University of Naples, in operation in 1944, showed that, from the afternoon of 22 March (14.00 coverage 03.10; 19.00 coverage 10/10) until the next day, the sky was completely covered with clouds from a height of about 1–2 km from the ground, thus making it difficult the observation of the eruptive column in all its development.

Adopting a numerical model of ash dispersion into the atmosphere, by using as input data both the dynamic parameters of the eruption and wind speed at various altitudes up to 12,000 m, we estimated that the eruptive column would reach a height of 10 km, higher than that previous supposed on the basis of the contemporary chronicles.

The last result justifies the dispersion of ash over wide areas as well as the extensive loss of livestock reported by the new witnesses accounts. The death of the sheep was probably the consequence of F (fluoride) poisoning (fluorosis) procured by the ingestion of grass, from pastures covered with ash, in analogy with what has been observed for other historical and contemporary eruptions in other parts of the world. The amount of F considered lethal to grazing animals is at least 100 μg/g body weight (NRC, 1974) (4–5 g for animals weighing 40–50 kg), while values close to 50 μg/g seem to be tolerated by sheep and cattle. We have measured F concentrations between 1500 and 3000 ppm in the 1944 Vesuvius volcanic ash. The obtained values indicate F content always higher than the lethality threshold; in fact, this F concentration in a layer of ash of even one mm thickness is sufficient to cause the death of the animals.

The 1944 deposit has been compared with those of other historical eruption as the Fuego 1974 and the Vesuvius 512 and 1906 AD deposits (e.g., Cole and Scarpati 2010); however for these events not much data are available on their environmental and human impacts. Thus to have an idea of the huge impact that a moderate eruption can have on the modern

society, an interesting parallel emerges between this historic eruption and that of the Eyjafjallajökull volcano in Iceland in April 2010, the most recent in Europe (Gudmundsson et al. 2010; Dellino et al. 2012; Cioni et al. 2014) that dispersed a moderate amount of ash over much of Europe.

Due to the significant impact on international air traffic and the implications on the vulnerability of modern society, the Eyjafjallajökull eruption has become a landmark event. The succession of phases, with the first fire-fountains and fissure-fed lava flows followed by explosive activity, the height of the eruption column (5–10 km), the duration of the paroxysmal phase with winds that pushed the ash to the SE, the volume of emitted products into the atmosphere ($5 * 10^6$ m^3), the average size of the clasts (40 μm) and the thickness of the deposit (~ 1 mm) to the Faroe Islands (a ~ 300 km away from the crater) are all comparable values with those related to the distal ash erupted during the paroxysm of Vesuvius in 1944. Of particular interest is the satellite view of the phenomenon in which it is possible to assess the extent of the ash cloud (>2000 km) that goes far beyond the limits of accumulation of products detected on the ground. However, the evolution of the eruption toward more explosive dynamics triggered by a sudden change in the composition of the magma and amplified by magma–water interaction processes/ash recycling (Iceland) and/or syn-eruptive crystallization (Vesuvius) characterizes both eruptions.

4 Conclusions

Our merged results on the 1944 eruption of Vesuvius, document the sudden increase in the degree of explosiveness during the middle phase (III mixed explosions) of the eruption, with the emission of a large amount of ash that was transported up to several hundred kilometers away from the volcano with strong impact on environment and people. In few hours, the eruption column reached a maximum height of at least 10 km on the crater, much greater than 5 km reported by the witnesses of the eruption due to the bad weather conditions preventing the direct observation of the eruptive cloud. Such sudden increase in the intensity of the volcanic scenario during ongoing eruptions, as shown by our study, should be taken into account as a precautionary measure for planning purposes. In fact, such a case of a moderate-intensity eruption of Vesuvius, similar to that which occurred in 1944, would be extremely disruptive, especially in our complex modern society.

References

Armienta MA, de La Cruz-Reyna S, Cruz O, Ceniceros N, Aguayo A, Marin M (2011) Fluoride in ash leachates: environmental implications at popocatepetl volcano, central Mexico. Nat Hazards Earth Syst Sci 11:1949–1956

Arrighi S, Principe C, Rosi M (2001) Violent strombolian and sub-plinian eruptions at Vesuvius during post-1631 activity. Bull Volcanol 63:126–150

Casertano L (1949) L'azione del vento su proietti vesuviani durante il parossismo del marzo 1944. Annali Osservatorio Vesuviano, V serie, volume unico, 381–395

Chester DK, Duncan AM, Wetton P, Wetton R (2007) Responses of the Anglo-American military authorities to the eruption of Vesuvius, March 1944. J Hist Geogr 33:168–196

Cioni R, Pistolesi M, Bertagnini A, Bonadonna C, Hoskuldsson A, Scateni B (2014) Insights into the dynamics and evolution of the 2010 Eyjafjallajökull summit eruption (Iceland) provided by volcanic ash textures. Earth Planet Sci Lett 394:111–123

Cole PD, Scarpati C (2010) The 1944 eruption of Vesuvius, Italy: combining contemporary accounts and field studies for a new volcanological reconstruction. Geol Mag 147:391–415

Cronin SJ, Neall VE, Lecointre JA, Hedley MJ, Loganathan P (2003) Environmental hazards of fluoride in volcanic ash: a case study from Ruapehu volcano, New Zealand. J Volcanol Geotherm Res 121:271–291

Cubellis E, Luongo G (1997) L'eruzione del marzo 1944. In Mons Vesuvius. Casa Editrice Fausto Fiorentino, Napoli, pp 273–294

Cubellis E, Marturano A (2010) Testimonianze, ricordi e descrizioni dell'ultima eruzione del Vesuvio del marzo 1944. Osservatorio Vesuviano-INGV, pp 42–214

Cubellis E, Marturano A (2014) Il Vesuvio e la guerra – Boati e fumo denso sul mare. Art. 33, n. 11–12, 31–35, ISSN:2280-4315, http://hdl.handle.net/2122/9757

Cubellis E, Marturano A, Pappalardo L (2013) Le ceneri distali dell'eruzione del Vesuvio del marzo 1944 raccolte a Devoli (Albania). Quaderni di Geofisica 113:37

Cubellis E, Marturano A, Pappalardo L (2014) L'Eruzione del Vesuvio del Marzo 1944: Testimonianze e Lettura Scientifica dell'Evento (L'Ambiente Antropico, vol III 2014)

Dawson J, Delbos E, Hough R, Lumsdon D, Mayes B, Watson H (2010) Impacts of volcanic ash originating from the April 2010 eruption in Eyjafjallajokull (Iceland) on the natural resources of Scotland. The Mcaulay Land Use Research Institute, Aberdeen

Del Moro A, Fulignati P, Marianelli P, Sbrana A (2001) Magma contamination by direct wall rock interaction: constraints from xenoliths from the walls of a carbonate-hosted magma chamber (Vesuvius 1944 eruption). J Volcanol Geotherm Res 112:15–24

Dellino P, Gudmundsson MT, Larsen G, Mele D, Stevenson JA, Thordarson T, Zimanowski B (2012) Ash from the Eyjafjallajökull eruption (Iceland): Fragmentation processes and aerodynamic behavior. J Geophys Res. doi:10.1029/2011JB008726

Fulignati P et al (2000) Glass-bearing felsic nodules from the crystallizing sidewalls of the 1944 Vesuvius magma chamber. Mineral Mag 64:481–496

Fulignati P, Marianelli P, Métrich N, Santacroce R, Sbrana A (2004) Towards a reconstruction of the magmatic feeding system of the 1944 eruption of Mt Vesuvius. J Volcanol Geotherm Res 133:13–22

Georgsson G, Pétursson G (1972) Fluorosis of sheep caused by the Hekla eruption in 1970. Fluoride 5:58–66

Ghiorso MS, Sack RO (1995) Chemical mass transfer in magmatic processes IV. A revised and internally consistent thermodynamic model for the interpolation and extrapolation of liquid–solid equilibria in magmatic systems at elevated temperatures and pressures. Contrib Mineral Petrol 119:197–212

Gudmundsson T et al (2010) Ash generation and distribution from the April–May 2010 eruption of Eyjafjallajökull, Iceland. Sci Rep 2:572. doi:10.1038/srep00572

Hazlett RW, Buesch D, Anderson JL, Elan R, Scandone R (1991) Geology, failure conditions, and implications of seismogenic avalanches of the 1944 eruption at Vesuvius, Italy. J Volcanol Geotherm Res 47(3):249–264

Imbò G (1945) Il parossismo vesuviano del marzo 1944. R. Acc. Sc. Fis. e Mat. della Soc. Reale di Napoli, Serie 4°, vol. XIII, pp 309–325

Imbò G (1949a) L'Osservatorio Vesuviano e le sue vicende durante il periodo bellico (1940–45)". Annali dell'Osservatorio Vesuviano, V Serie, vol. unico, 1949. Published on 30 June 1951

Imbò G (1949b) L'attività eruttiva vesuviana e relative osservazioni nel corso dell'intervallo eruttivo 1906–1944 ed in particolare del parossismo del marzo 1944. Annali dell'Osservatorio Vesuviano, V Serie, vol. unico, 1949. Published on 30 June 1951

Imbò G (1952) Sismicità del Parossismo Vesuviano del Marzo 1944. Annali Osservatorio Vesuviano, Naples

Imbò G (1956). Sul dinamico riposo del Vesuvio. Annali dell'Osservatorio Vesuviano, vol. secondo: 79–94

Lazzari A (1948) Segnalazione della caduta in Albania delle ceneri del Vesuvio dell'eruzione del Marzo 1944. Bollettino Società dei Naturalisti di Napoli 57:3–6

Lazzari Francesco de Sio (2013) Antonio Lazzari dall'Albania alla Val d'Agri. Sito Associazione Pionieri e Veterani ENI (Apve) http://www.pionierieni.it/wp/wp content/uploads/Ricordo-del-geologo-Antonio-Lazzari.-Di-F-Lazzari.pdf

Lazzari Francesco de Sio (2014) Un geologo umanista: Antonio Lazzari (1905–1979). L'Ambiente Antropico, n. 5, pp 74–87. ISSN:2282-823X

Le Bas MJ, Le Maitre RW, Streckeisen A, Zanettin B (1986) A chemical classification of volcanic rocks based on the total alkali–silica diagram. J Petrol 27:745–750

Lima A, De Fedele L, Sintoni MF (2006) Influence of hydrothermal processes on geochemical variations between 79 AD and 1944 AD Vesuvius eruptions. In: De Vivo B (ed) Volcanism in the Campania Plain: Vesuvius, Campi Flegrei and Ignimbrites. Developments in volcanology 9. Elsevier, New York, pp 235–247

Lima A, De Vivo B, Fedele L, Sintoni MF, Milia A (2007) Geochemical variations between the 79 AD and 1944 AD Somma-Vesuvius volcanic products: constraints on the evolution of the hydrothermal system based on fluid and melt inclusions. Chem Geol 237:401–417

Macedonio G, Costa A, Folch A (2008) Ash fallout scenarios at Vesuvius: numerical simulation and implications for hazard assessment. J Volcanol Geotherm Res 148:366–377

Marianelli P, Metrich N, Sbrana A (1999) Shallow and deep reservoirs involved in magma supply of the 1944 eruption of Vesuvius. Bull Volcanol 61:48–63

Marianelli P, Sbrana A, Métrich N, Cecchetti A (2005) The deep feeding system of Vesuvius involved in recent violent strombolian eruptions. Geophys Res Lett 32:L02306

Marziano GI, Schmidt CB, Dolfi D (2007) Equilibrium and disequilibrium degassing of a phonolitic melt (Vesuvius AD 79 "white pumice") simulated by decompression experiments. J Volcanol Geotherm Res 161(3):151–164

Mastrolorenzo G, Pappalardo L, Troise C, Panizza A, De Natale G (2008) Probabilistic tephra hazard maps for the Neapolitan area: quantitative volcanological study of Campi Flegrei eruptions. J Geophys Res 113:B07203. doi:10.1029/2007JB004954

Morgan DJ, Blake S, Rogers NW, DeVivo B, Rolandi G, Macdonald R, Hawkeswothd CJ (2004) Time scales of crystal residence and magma chamber volume from modelling of diffusion profiles in phenocrysts: Vesuvius 1944. Earth Planet Sci Lett 222:933–946

Morimoto N (1988) Nomenclature of pyroxenes. Am Mineral 73:1123–1133

National Academy of Sciences—National Research Council Committee on Animal Nutrition, Subcommittee on Fluorosis (1974) Effects of fluoride on animals. US National Academy of Sciences, Washington

Pappalardo L, Mastrolorenzo G (2010) Short residence times for alkaline Vesuvius magmas in a multi-depth supply system: evidence from geochemical and textural studies. Earth Planet Sci Lett 296:133–143

Pappalardo L, Piochi M, Mastrolorenzo G (2004) The 3550 YR BP-1944 AD magma-plumbing system of Somma-Vesuvius: constraints on its behavior and present state through a review of Sr-Nd isotope data. Ann Geophys 47:1471–1483

Pappalardo L, D'Auria L, Cavallo A, Fiore S (2014) Petrological and seismic precursors of the paroxysmal phase of the last Vesuvius eruption on March 1944. Scientific Reports 4, Article number: 6297. doi:10.1038/srep06297

Parascandola A (1945) L'eruzione vesuviana del marzo 1944, i prodotti piroclastici. Rendiconti Accademia Scienze Fisiche Matematiche di Napoli, Serie IV 13:285–305

Parascandola A (1948) Se sia stato esclusivamente terminale l'afflusso lavico nella eruzione vesuviana del marzo 1944. Bollettino Societa dei Natataralisti di Napoli 56:141–164

Pesce A, Rolandi G (1994) Vesuvio 1944. L'ultima eruzione. S. Sebastiano al Vesuvio, 1944

Pfeiffer T, Costa A, Macedonio G (2005) A model for the numerical simulation of tephra fall deposits. J Volcanol Geotherm Res 140:273–294

Pichavant M, Scaillet B, Pommier A, Iacono-Marziano G, Cioni R (2014) Nature and evolution of primitive Vesuvius magmas: an experimental study. J Petrol 55(11):2281–2310

Romano S (2011) Quella eruzione del Vesuvio mentre l'Europa è in guerra. Corriere della Sera 26(5):2011

Santacroce R (1987) Somma Vesuvius. Quaderni de "La Ricerca Scientifica" del CNR 114, vol. 8

Scandone R, Iannone F, Mastrolorenzo G (1986) Stima dei parametri dinamici dell'eruzione del 1944 del Vesuvio. Atti Convegno GNV, pp 487–512

Scandone R, Giacomelli L, Fattori Speranza F (2008) Persistent Activity and Violent Strombolian Eruptions at Vesuvius between 1631 and 1944. J Volcanol Geotherm Res 170:167–180

Scherillo A (1949) Le lave e le scorie dell'eruzione vesuviana del 1944. Annali Osservatorio Vesuviano 5:169–184

Scherillo A (1953) Nuovo contributo allo studio dei prodotti dell'eruzione vesuviana del 1944. Bull Volc 13:129–144

Shea T, Larsen JF, Gurioli L, Hammer JE, Houghton BF, Cioni R (2009) Leucite crystals: surviving witnesses of magmatic processes preceding the 79AD eruption at Vesuvius, Italy. Earth Planet Sci Lett 281:88–98

Signorelli S, Carroll MR (2000) Solubility and fluid-melt partitioning of Cl in hydrous phonolitic melts. Geochim Cosmochim Acta 64(16):2851–2862

Thorarinsson S (1979) On the damage caused by volcanic eruptions with special reference to tephra and gases. In: Sheets PD, Grayson DK (eds) Volcanic activity and human ecology. Academic Press, New York, pp 125–159

Trigila R, De Benedetti A (1993) Petrogenesis of Vesuvius historical lavas constrained by Pearce element ratios analysis and experimental phase equilibria. J Volcanol Geotherm Res 58:315–343

Ventura G, Vilardo G (2008) Emplacement mechanism of gravity flows inferred from high resolution Lidar data: The 1944 Somma-Vesuvius lava flow (Italy). Geomorphology 95:223–235

Vilardo G, Ventura G (2008) Geomorphological map of the 1944 Vesuvius lava flow (Italy). J Maps 2008: 225–234. http://www.journalofmaps.com

Villemant B, Trigila R, De Vivo B (1993) Geochemistry of Vesuvius volcanics during 1631–1944 period. J Volcanol Geotherm Res 58:291–313